

# Generation Meets Verification: Accelerating Large Language Model Inference with Smart Parallel Auto-Correct Decoding

Hanling Yi<sup>1</sup>, Feng Lin<sup>1,2</sup>, Hongbin Li<sup>1</sup>, Peiyang Ning<sup>1</sup>, Xiaotian Yu<sup>1</sup>, Rong Xiao<sup>1</sup>

<sup>1</sup>Intellifusion Inc.

<sup>2</sup>Harbin Institute of Technology, Shenzhen

{hanling.cuhk, lee.blingner, ningpeiyang,  
xiaotianyu.ac, rongxiao}@gmail.com  
lin1993@mail.ustc.edu.cn

## Abstract

This research aims to accelerate the inference speed of large language models (LLMs) with billions of parameters. We propose Smart Parallel Auto-Correct dEcoding (SPACE), an approach designed for achieving lossless acceleration of LLMs. By integrating semi-autoregressive inference and speculative decoding capabilities, SPACE uniquely enables autoregressive LLMs to parallelize token generation and verification. This is realized through a specialized semi-autoregressive supervised fine-tuning process that equips existing LLMs with the ability to simultaneously predict multiple tokens. Additionally, an auto-correct decoding algorithm facilitates the simultaneous generation and verification of token sequences within a single model invocation. Through extensive experiments on a range of LLMs, SPACE has demonstrated inference speedup ranging from 2.7x-4.0x on HumanEval-X while maintaining output quality.

## 1 Introduction

The majority of large language models (LLMs), including prominent examples like ChatGPT (Brown et al., 2020) and LLaMA (Touvron et al., 2023), are autoregressive (AR) in nature. During the inference stage, these AR models generate tokens one by one in a sequential manner. This sequential approach limits parallelism, leading to underutilization of modern parallel computing resources such as GPUs. Consequently, the inference stage becomes memory-bound and the inference latency increases noticeably, particularly with advanced LLMs boasting billions of parameters.

A straightforward method to mitigate the latency is to adapt the model to predict multiple future tokens in parallel. Such models are commonly referred to as semi-autoregressive (SAR) models (Wang et al., 2018). Nonetheless, the vast majority of LLMs are inherently AR and, hence, unable to perform inference in a SAR manner. In

addition, SAR models commonly experience a deterioration in the output quality due to their parallel decoding nature (Xiao et al., 2023). Furthermore, it is worth mentioning that pretraining any LLM from scratch is computationally expensive.

Another effective way to speed up AR sampling is speculative decoding (Leviathan et al., 2023; Chen et al., 2023; Miao et al., 2023). Speculative decoding typically adheres to the ‘draft-then-verify’ paradigm, wherein multiple candidate tokens are initially generated by fast-to-infer smaller models, and are subsequently validated in parallel by the larger LLM. This validation process, based on rejection sampling, ensures that the final output is consistent with the LLM’s distribution, thereby achieving lossless speedup. Nonetheless, speculative decoding is contingent on the availability of smaller models, which must utilize the same tokenizer as the larger model to function properly.

Integrating SAR inference with speculative decoding presents a promising approach to accelerate language model inference. By adapting a model to autonomously generate and validate a sequence of future tokens, we establish an efficient and self-reliant process that greatly enhances the speed of inference. This union yields substantial practical benefits: it eliminates the requirement for smaller auxiliary models, thereby simplifying the overall implementation and reducing memory overhead during inference. Furthermore, by shifting the emphasis away from precise prediction of multiple tokens towards speculative generation followed by verification, the difficulty of the SAR training phase can be significantly reduced.

In this paper, we propose Smart Parallel Auto-Correct dEcoding (SPACE), a approach that allows LLMs to generate multiple tokens speculatively while simultaneously verifying them. SPACE harmonizes a SAR model with a draft-then-verify inference algorithm to optimize inference speed while maintaining high model quality. We demon-

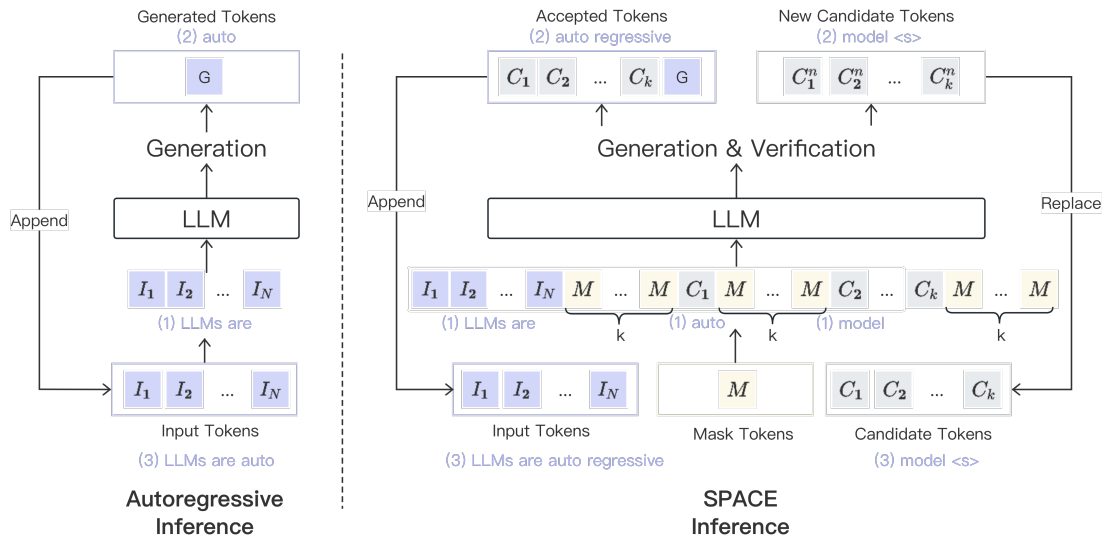


Figure 1: A visual comparison between conventional AR inference (left) and SPACE inference (right) is illustrated. In AR inference, token generation proceeds in a sequential manner, with only one token output per decoding step. In SPACE inference, the input token sequence (i.e., “LLMs are”) is augmented with  $k + 1$  groups of mask tokens and  $k$  candidate tokens (i.e., “auto” and “model”). The candidate tokens undergo verification to obtain accepted tokens (i.e., “auto” and “regressive”), and  $k$  new candidate tokens (i.e., “model” and “<s>”) are generated from one of the mask groups after a single model invocation. An illustration of the generation and verification process can be found in Figure 2. SPACE allows for a variable number of tokens to be generated in each step, with the quantity ranging from a minimum of 1 to a maximum of  $k + 1$ .

strate that an AR language model can be adapted to produce probable token sequences in parallel through semi-autoregressive supervised fine-tuning (SAR-SFT). This strategy obviates the need for supplementary models and maintains the fine-tuning process within reasonable computational demands. We also introduce an auto-correct decoding algorithm that enables the generation and validation of token candidates to occur concurrently within a single invocation of a model, thereby significantly boosting inferential efficiency. SPACE is particularly useful for edge server applications of LLMs, where it can effectively utilize the computing resources to accelerate the inference speed in low batch size scenarios. A visual comparison between AR and SPACE inference can be found in Figure 1. Our key contributions are summarized as follows:

- We propose a SAR-SFT scheme that empowers autoregressive LLMs to generate multiple tokens at once, without requiring substantial computational overhead.
- We introduce an auto-correct decoding algorithm that facilitates the concurrent generation and validation of candidate tokens within a single forward pass of the model.
- Our extensive experiments, conducted across

various LLMs with parameters ranging from 6B to 70B, validate that SPACE is effective in achieving an inference speedup from 2.7x to 4.0x in HumanEval-X while maintaining output quality.

## 2 Related Work

**Speculative Decoding** Speculative decoding (Leviathan et al., 2023; Chen et al., 2023) accelerates LLM inference by using a smaller draft model to predict larger target model outputs, with subsequent verification by the target model. The efficacy of the method is contingent on the accuracy of the draft model’s predictions. To enhance accuracy, researchers have adopted various strategies such as employing ensembles of boosted draft models (Miao et al., 2023), staged draft models (Spector and Ré, 2023), retraining the target model with addition of auxiliary prediction heads (Stern et al., 2018), introducing advanced coordination policies (Kim et al., 2023) and refining the decoding algorithm (Sun et al., 2023; Lin et al., 2024). However, speculative decoding hinges on the accessibility of suitable smaller models, which can be difficult to obtain and often requiring extra training and careful tuning (Liu et al., 2023). SPACE circumvents this challenge

by fine-tuning the target model to prognosticate future token sequences in parallel, eliminating the dependency on extra small model.

Recent advancements like Lookahead Decoding (Fu et al., 2023) and Self-Speculative (Zhang et al., 2023) have refined the draft-then-verify process, forgoing the need for extra models or intricate training steps. Although simpler, these methods tend to provide less acceleration than SPACE. Contrarily, Medusa (Cai et al., 2024) and PaSS (Monea et al., 2023) leverage fine-tuning of a single LLM to perform both token generation and validation. PaSS, through fine-tuning lookahead token embeddings, allows LLMs to predict multiple tokens ahead, but with a limited speedup of about 30% as their verification and drafting phases occur sequentially. Medusa adds multiple decoding heads to the LLM and introduces a tree-based decoding algorithm for faster inference, but it struggles with larger batch sizes owing to the increased computational demands of tree-structured attention.

**Semi-Autoregressive Decoding** SAR departs from the AR approach by decoding multiple tokens in parallel, thereby significantly enhancing inference efficiency. Particularly in machine translation, SAR has achieved a fivefold speed increase while preserving 88% of the model quality (Wang et al., 2018). For SAR decoding, it is a common trick to employ mask tokens as placeholders in input. This approach, originating from the mask-predict paradigm introduced by Ghazvininejad et al. in machine translation, has since become a widely recognized decoding strategy (Xiao et al., 2023). Inspired by this paradigm, SPACE adopts  $k$  mask tokens to predict  $k$  future tokens. Xia et al. accelerate inference of an AR model by creating draft tokens with a SAR model and then refined by the AR model. Unlike their method which necessitates a secondary SAR model for draft generation, SPACE eliminates this requirement, merging generation and verification phases for enhanced efficiency.

### 3 Methods

SPACE primarily comprises two components: the SAR-SFT scheme and the auto-correct decoding algorithm. The SAR-SFT scheme enhances an autoregressive LLM’s capacity for speculative multi-token generation in a single decoding step. Meanwhile, the auto-correct decoding algorithm allows the LLM to concurrently generate and verify candidate tokens. We introduce the details of these two

components in the following subsections.

#### 3.1 Semi-Autoregressive Finetuning

Conventionally a pretrained LLM undergoes a process known as supervised fine-tuning (SFT) to adapt the model to specific downstream tasks. Specifically, given the prompt token sequence  $X$  and the answer token sequence  $Y = \{y_1, y_2, \dots, y_N\}$ , the AR model is trained in SFT with loss function

$$\mathcal{L}_{AR} = - \sum_{t=1}^N \log P(y_t | y_{<t}, X; \theta), \quad (1)$$

where  $y_t$  is the token to be predicted at step  $t$ ,  $y_{<t}$  is the tokens predicted in previous  $t - 1$  decoding steps and  $\theta$  is the model parameters.

In the proposed SAR-SFT scheme, our objective is to train the model to generate  $k$  consecutive tokens when presented with an input sequence containing  $k$  mask tokens. The adaptation from traditional SFT to SAR-SFT affects only the dataloader component in implementation. In this modified dataloader, each data sample remains unchanged with a probability  $p_{ar}$ . Conversely, with a probability of  $1 - p_{ar}$ , we randomly select a position  $m$  from  $\{0, 1, \dots, N - k\}$  in the input sequence to replace  $k$  consecutive tokens with mask tokens. We then truncate the input token sequences to keep the first  $m + k$  tokens, denoted as  $y_{<m}^k$ :

$$y_{<m}^k = \{y_1, y_2, \dots, y_{m-1}, \underbrace{[M], \dots, [M]}_{\times k}\}. \quad (2)$$

Under this modified dataloader, with probability  $p_{ar}$  the model is trained with the original AR loss  $\mathcal{L}_{AR}$ . With probability  $1 - p_{ar}$ , the model is trained with the SAR loss function defined as follows:

$$\mathcal{L}_{SAR} = - \sum_{t=1}^{m-1} \log P(y_t | y_{<t}, X; \theta) - \sum_{t=m}^{m+k} \log P(y_t | y_{<m}^k, X; \theta) \quad (3)$$

Intuitively, the hyper-parameter  $p_{ar}$  plays a critical role in striking a balance between the AR loss and the SAR loss. By selecting an appropriate value for  $p_{ar}$ , the LLM is trained not only to adhere to downstream tasks but also to predict multiple tokens at each decoding step.

We note that the primary goal of SAR-SFT is not to compel the LLM to predict several tokens

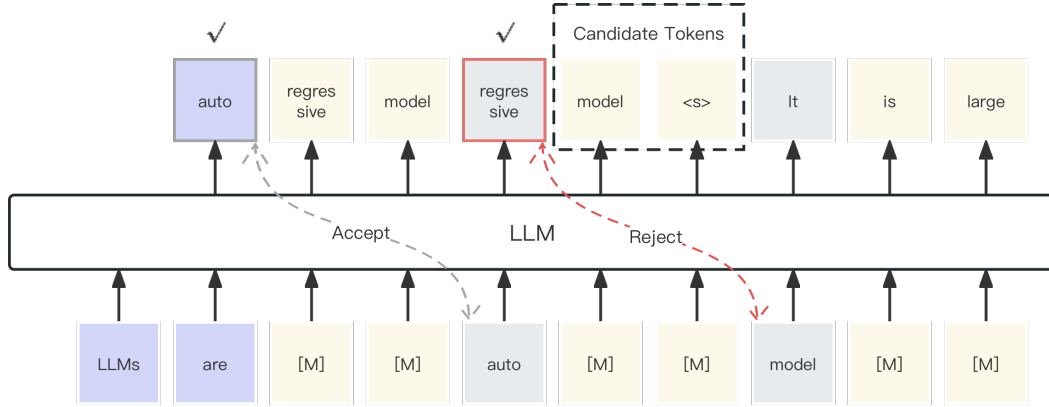


Figure 2: An illustrative example of the auto-correct decoding algorithm in SPACE. In this example, the first candidate token “auto” is accepted, while the second candidate token “model” is rejected. The LLM generates two new tokens “auto” and “regressive” in this decoding step and two new candidate tokens “model” and “<s>” from the second mask group.

in parallel with high accuracy, as this can be an exceedingly challenging task. Rather, our goal is to enable the LLM to make an “educated guess” about the upcoming few tokens, which is more attainable. This strategy allows the model to improve its inference efficiency by preparing probable token sequences beforehand, which can later be validated and refined by the auto-correct decoding algorithm introduced in next subsection.

### 3.2 Auto-Correct Decoding Algorithm

Unlike previous methods (Leviathan et al., 2023; Chen et al., 2023) that rely on auxiliary models, SPACE streamlines the process by using the same LLM for generation and subsequent verification of candidate tokens. To enhance inference efficiency, we have developed an algorithm that enables this unified LLM to concurrently verify tokens from the current step and generate new candidates for the next step within a single forward pass.

Algorithm 1 outlines the auto-correct decoding algorithm employed in SPACE, with Figure 2 providing an illustrative example. When presented with an initial prompt (e.g., “LLMs are”) alongside  $k$  candidate tokens (e.g., “auto” and “model”), the algorithm begins by constructing an input token sequence. This is achieved by augmenting the original prompt with  $k + 1$  groups of mask tokens, interspersed with the  $k$  candidate tokens, as depicted in Figure 2. Specialized attention masks and positional indices are devised to constrain the influence of the mask tokens, allowing them to “see” only preceding non-mask tokens and other mask

---

#### Algorithm 1 The auto-correct decoding algorithm

---

**Input:** A sequence of input tokens  $\mathcal{T}$ , number of mask tokens  $k$ , large language model  $\mathcal{M}$

**Output:** A sequence of generated tokens  $\mathcal{O}$

- 1:  $\mathcal{O} = \mathcal{T}$ ,  $L_c = [0] \times k$ ,  $P_c = [+∞] \times k$
  - 2: **while** True **do**
  - 3:      $l = \text{len}(\mathcal{O})$
  - 4:     Get  $\mathcal{I}$ ,  $\bar{A}$ ,  $\bar{P}$  according to equation (4)-(5)
  - 5:      $P = \mathcal{M}(\mathcal{I}, \bar{A}, \bar{P})$    ▷ Get the output logits
  - 6:      $idx = l + 1$
  - 7:      $Q = P[l]$    ▷ The logit of the  $l$ -th token
  - 8:     **for**  $i = 1$  to  $k$  **do**
  - 9:          $r \sim U(0, 1)$
  - 10:         **if**  $r \leq Q(L_c[i])/P_c[i]$  **then**
  - 11:              $\mathcal{O}.\text{append}(L_c[i])$
  - 12:              $idx = idx + k + 1$
  - 13:              $Q = P[l + i * (k + 1)]$
  - 14:         **else**
  - 15:             **break**
  - 16:         **end if**
  - 17:     **end for**
  - 18:      $a \sim Q$    ▷ Sample one extra token
  - 19:      $\mathcal{O}.\text{append}(a)$
  - 20:     **if** <EOS> in  $\mathcal{O}$  **then**
  - 21:         return  $\mathcal{O}[:\text{eos\_index}]$
  - 22:     **end if**
  - 23:      $L_c \sim P[idx : idx + k]$    ▷ New candidates
  - 24:      $P_c = P[idx : idx + k](L_c)$    ▷ Probability
  - 25: **end while**
-



tokens within their respective groups. Following a forward pass through the LLM, a verification step is applied to the candidate tokens. If  $i^*$  tokens (where  $0 \leq i^* \leq k$ ) pass this check, the algorithm proceeds to generate  $k$  new candidate tokens (e.g., “model” and “<s>”) from the  $(i^* + 1)$ -th mask group and one extra token from the  $i^*$ -th candidate token (e.g., “regressive”). In this case,  $i^* + 1$  new tokens are generated from a single LLM forward step.

In the following, we introduce the auto-correct decoding algorithm in details. Given a sequence of input prompt tokens  $\mathcal{T} = \{x_1, x_2, \dots, x_l\}$  and a list of  $k$  candidate tokens  $L_c = \{c_1, c_2, \dots, c_k\}$  generated from the previous decoding step, we first construct a sequence of input tokens  $\mathcal{I}$  as follows:

$$\mathcal{I} = \{x_1, \dots, x_l, L_m^k, c_1, L_m^k, \dots, c_k, L_m^k\}, \quad (4)$$

where  $L_m^k = \underbrace{[M], \dots, [M]}_{\times k}$  represents a group of  $k$  mask tokens and there are  $k + 1$  groups of them in  $\mathcal{I}$ . The sequence  $\mathcal{T}$  is expanded by  $k \cdot (k + 2)$  additional tokens, resulting in a total length of  $|\mathcal{I}| = l + k \cdot (k + 2)$ . These  $k + 1$  groups of mask tokens are designated for the generation of new candidate tokens.

Since LLM decoding is primarily bounded by memory bandwidth, we can merge the generation and verification in the same forward step, leveraging GPU’s parallel processing power to hide overheads. We achieve this by designing special attention mask  $\bar{A} \in \{0, 1\}^{|\mathcal{I}| \times |\mathcal{I}|}$  as follow:

$$\bar{A}_{ij} = \begin{cases} 1 & i \geq j, \mathcal{I}[j] \neq M \\ 1 & i \geq j, i - j < k, \mathcal{I}[i] = \mathcal{I}[j] = M \\ 0 & \text{otherwise} \end{cases} \quad (5)$$

An illustrative example of the attention mask configuration is depicted in Figure 7 in Appendix A.3. The positional indices for positional encoding can be computed as  $\bar{P}_i = \sum_{j=1}^{|\mathcal{I}|} \bar{A}_{ij} - 1$ .

Following the input construction phase, we proceed with the inference process using the LLM, from which we derive the normalized output logits, denoted as  $P$ . The candidate tokens are then verified through rejection sampling, which is detailed from Line 6 to Line 22 in Algorithm 1. Denote  $P_c$  as the list of semi-autoregressive probability of candidate tokens obtained from the previous step. Formally  $P_c[i]$  is defined as:

$$P_c[i] = P(c_i | x_1, \dots, x_{l-1}, \underbrace{[M], \dots, [M]}_{\times i}) \quad (6)$$

Denote  $Q_c$  as the list of autoregressive probability of candidate tokens from the current step <sup>1</sup>.

$$Q_c[i] = P(c_i | x_1, \dots, x_l, c_1, \dots, c_{i-1}) \quad (7)$$

Starting from  $i = 1$ , we accept token  $c_i$  with probability  $\min(1, \frac{Q_c[i]}{P_c[i]})$ . Upon acceptance of token  $c_i$ , the algorithm output  $c_i$  and proceeds to validate the subsequent token  $c_{i+1}$  using the same criterion; conversely, if  $c_i$  is rejected, the verification process terminates immediately and one extra token is generated from the output logit of the last accepted candidate token, as shown in Line 18 in Algorithm 1. It is important to observe that during each decoding step, the number of generated tokens ranges from a minimum of one to a maximum of  $k + 1$ . By employing rejection sampling, it can be proved that the distribution of the output token sequence matches that of the AR inference process in the LLM. For a more comprehensive explanation of this claim, readers can refer to prior research (Leviathan et al., 2023; Chen et al., 2023).

## 4 Experiments

### 4.1 Experimental Settings

**Training** We conduct experiments on LLMs with various sizes, including ChatGLM3-6B-Base (Du et al., 2022), LLaMA-2 (7B, 13B, 70B) (Touvron et al., 2023), Qwen-14B (Bai et al., 2023), InternLM-20B (Team, 2023), Falcon-40B (Almazrouei et al., 2023). To ensure reproducibility, we finetune the models using publicly available SFT datasets, including Alpaca-GPT4 (Peng et al., 2023), Lima (Zhou et al., 2023), Oaast-SFT (LAION-AI, 2023), CodeAlpaca (Chaudhary, 2023), and OpenPlatypus (Lee et al., 2023). The details of these datasets are listed in Table 5 in Appendix A.1. There are in total 166,993 training samples. We add the mask token as a special token and initialize its embedding with normal distribution. Unless otherwise specified, we set the number of mask tokens  $k = 5$  and  $p_{\text{ar}} = 0.5$ . The training details can be found in Appendix A.1.

**Inference** In our assessment of SPACE, we employ four distinct datasets: Chatbot Instruction Prompt (CIP) (Palla, 2023), MT-Bench (Zheng et al., 2023a), HumanEval-X (Zheng et al., 2023b) and XSum (Narayan et al., 2018). For inference baseline, we train LLMs with SFT under the same

<sup>1</sup>By definition,  $Q_c[i]$  is equivalent to  $Q(L_c[i])$  in Line 10 of Algorithm 1.

datasets and training configuration used for SAR-SFT. We adopt the generation algorithm provided by the Huggingface Transformers library (Wolf et al., 2020), executing it in an autoregressive fashion on the SFT model. We conduct the experiments on a server with eight A800 (80GB) GPUs. By default, we set the batch size to 1 during inference. To evaluate the inference efficiency of SPACE, we employ two metrics: speedup and average accepted tokens. The speedup metric is defined as the ratio of the inference speed of the baseline method (measured in tokens per second) to the inference speed achieved using SPACE. The second metric, average accepted tokens, is computed as the ratio of the total number of tokens generated to the number of inference steps performed by the LLM. The evaluation details can be found in Appendix A.2.

## 4.2 Experimental Results

### 4.2.1 Inference Efficiency

The experimental results on XSum, HumanEval-X and CIP under greedy sampling setting are shown in Table 1. We observe that SPACE predominantly corresponds closely with baseline performance levels in both the XSum and HumanEval-X benchmarks. Moreover, SPACE demonstrably realizes a speedup in the range of 1.5 to 4.0, depending on the models and datasets. The maximal acceleration, seen in LLaMA-2-70B on HumanEval-X, clocks in at an impressive 4.04. More experimental results of SPACE under random sampling can be found in Appendix A.4.

From the above results, we have the following three observations: First, SPACE consistently achieves speedup while maintaining performance comparable to the baseline across models of varying sizes, showcasing its broad applicability. Specifically, the results attained by SPACE in tasks such as XSum and HumanEval-X closely mirror those achieved by the baseline method, as indicated by the comparable performance metrics listed in parentheses in Table 1.

Second, the magnitude of speedup experienced is model-specific, indicating that the efficiency benefits of SPACE can differ in models. This variance might stem from several factors: (1) the models’ vocabularies vary, with less efficient vocabularies possibly leading to greater predictability and thus higher speedup; and (2) models with more parameters often enjoy more substantial speedup, likely owing to their superior predictive capabilities that

facilitate earlier anticipation of forthcoming tokens.

Lastly, when applying SPACE to different tasks, the same model can exhibit dramatically different speedup ratios. In particular, tasks that involve programming, such as those in the HumanEval-X benchmark, exhibit the most significant speedup, achieving an average rate of 3.33 using greedy sampling. This observation aligns with the results in previous research (Chen et al., 2023), and could be attributed to the inherently structured and predictable nature of programming code.

To ensure a fair and unbiased comparison, we have reproduced several accelerating methods, such as self-speculative decoding (Zhang et al., 2023), look-ahead decoding (Fu et al., 2023), assistant generation from HF (Joao Gante, 2023) and speculative decoding (Leviathan et al., 2023). All experiments were executed on the MT-Bench dataset using identical hardware configurations in conjunction with the LLaMA-2-70B model. According to the outcomes presented in Table 2, SPACE outperforms other methods by achieving the highest speedup. This demonstrates the competitiveness of SPACE in inference acceleration.

### 4.2.2 Impact of SAR-SFT on Model Quality

While SPACE accelerates inference speed, it is imperative to explore whether LLMs trained with SAR-SFT suffer performance degradation compared to those trained with the conventional SFT approach. To this end, we train LLMs with SFT under the same datasets and training configuration used for SAR-SFT. Note that by setting  $p_{ar} = 1$ , SAR-SFT effectively becomes equivalent to SFT.

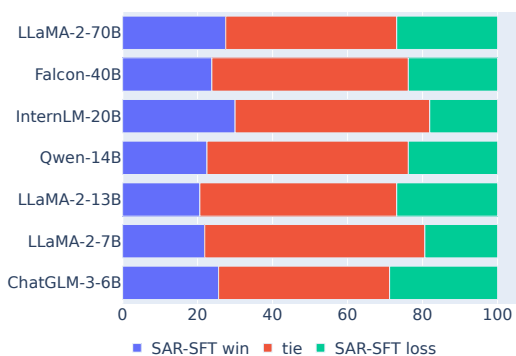


Figure 3: Win rate comparison in MT-Bench: SAR-SFT versus SFT judged by GPT-4. Best viewed in color.

Model	XSum			HumanEval-X			CIP	
	ROUGE-L	Avg. Tokens	Speed-up	Pass@10	Avg. Tokens	Speed-up	Avg. Tokens	Speed-up
ChatGLM-3-6B	14.5 (14.3)	2.04	1.48	18.3 (18.3)	3.34	2.71	1.80	1.52
LLaMA-2-7B	16.0 (16.1)	2.23	1.92	18.9 (18.9)	3.54	3.18	1.85	1.72
LLaMA-2-13B	15.1 (15.0)	2.36	2.08	20.1 (20.1)	3.76	3.43	1.99	1.82
Qwen-14B	17.2 (17.2)	2.15	1.94	26.8 (26.8)	3.51	3.19	1.85	1.68
InternLM-20B	16.4 (16.3)	2.15	1.99	21.3 (21.3)	3.31	3.16	1.80	1.63
Falcon-40B	15.7 (15.8)	2.17	2.03	20.7 (20.7)	3.58	3.58	1.96	2.02
LLaMA-2-70B	16.4 (16.3)	2.54	2.34	28.0 (28.0)	4.32	4.04	2.09	1.89

Table 1: The experimental results on XSum, HumanEval-X and CIP under greedy sampling setting. We show the average accepted tokens (Avg. Tokens) and inference speedup (Speedup) for each datasets. The number in parentheses shows the corresponding results of the baseline method.

Method	Speedup
Self-SpecDec (Zhang et al., 2023)	1.15
Look-ahead (Fu et al., 2023)	1.22
HF AssistGen (Joao Gante, 2023)	1.53
SpecDec (Leviathan et al., 2023)	1.79
SPACE (ours)	2.26

Table 2: Comparison of speedup for various acceleration methods with LLaMA-2-70B on MT-Bench dataset.

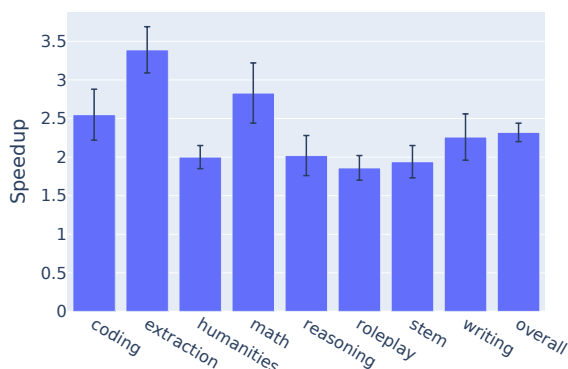


Figure 4: The mean and standard deviation of speedup for all models under greedy sampling setting in MT-Bench.

For a comprehensive comparison, MT-Bench was employed with GPT-4 serving as the evaluator to measure the performance disparity between the LLMs trained with the two training schemes. The results are presented in Figure 3. We can observe that models trained with SAR-SFT scheme have comparable performance as compared to their SFT counterparts. Specifically, the majority of questions assessed in MT-Bench ended in a deadlock across all models, implying that training an LLM with SAR-SFT does not deteriorate the model’s quality.

Additionally, SAR-SFT-trained models have exhibited advantages in speed. The mean and standard deviation of the speedup for all models in various tasks within MT-Bench are shown in Figure 4. It becomes evident that the speedup ratios vary considerably across different tasks, with the highest gains observed in tasks related to extraction, math, and coding. On average, all the models achieved a speedup ratio of 2.3 in MT-Bench dataset. More details can be found in Table 6 in the appendix.

To further validate that SAR-SFT does not compromise the model’s effectiveness, a comprehensive evaluation was conducted using a suite of widely adopted benchmarks, including MMLU, BoolQ, and others. More detailed can be found in Appendix A.5.

### 4.2.3 Ablation Study

Our ablation study investigates the impact of varying the number of masked tokens, denoted as  $k$ , on the speedup ratio of the LLaMA-2-7B model using the MT-Bench dataset. The results of this analysis are presented in Figure 5. Our findings indicate that a setting of  $k = 5$  achieves an optimal balance for the model’s performance. During the SAR-SFT phase, the LLM is tasked with concurrently predicting a sequence of  $k$  subsequent tokens. Increasing the value of  $k$  elevates the complexity of the prediction task and introduces computational overhead during inference, which may inversely correlate with the acceleration of the decoding process. Conversely, setting too low a value for  $k$  leads to an underutilization of the model’s capacity for parallel decoding, potentially resulting in a less pronounced improvement in decoding speed.

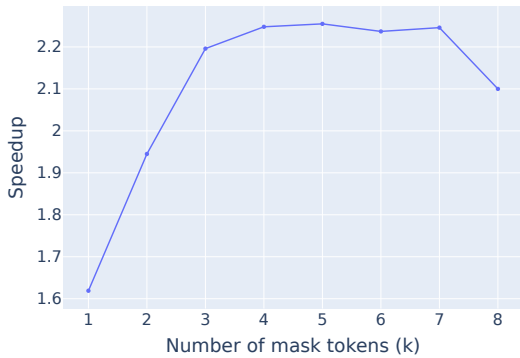


Figure 5: Ablation study on number of mask tokens based on LLaMA-2-7B. The speedup is evaluated under greedy sampling setting on MT-Bench dataset.

### 4.3 Integration with TGI

When deploying LLMs for production use, it’s common to leverage advanced LLM serving engines designed to enhance the efficiency of text generation tasks. The Text Generation Inference (TGI) (HuggingFace, 2023) framework is one such example, widely recognized for its support for a suite of acceleration techniques such as flash attention, tensor parallelism, and continuous batching.

We have integrated SPACE with the TGI framework. The primary objective of this integration is to ascertain whether SPACE can yield acceleration gains even when combined with other advanced inference-optimizing techniques presented in TGI. The results shown in Figure 6 were encouraging: with SPACE, TGI achieved a speed increase ranging from 1.5x to 3.4x across various model sizes. Remarkably, the incorporation of SPACE enabled LLaMA-2-13B model to reach inference speeds comparable to, if not surpassing, those of a 7 billion-parameter model without SPACE supports.

To assess SPACE’s efficacy with larger batch sizes, we carried out experiments on the MT-Bench dataset using the LLaMA-2-70B model through TGI. The results in Table 3 suggest a reduced speedup from SPACE as batch sizes grow. Notably, SPACE with five masks ( $k = 5$ ) achieves only a 1.39x improvement with a batch size of 16. This diminishing speedup is due to the computational overhead introduced by the additional tokens during the inference phase, an effect that is magnified as batch size escalates. Additionally, our findings indicate that decreasing the number of masks enhances SPACE performance. Specifically

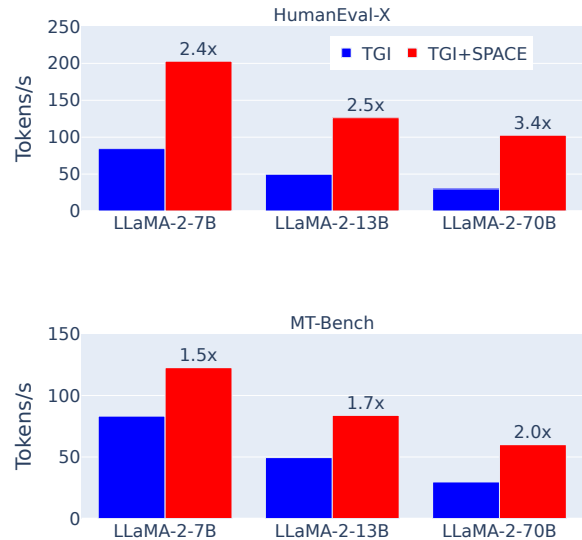


Figure 6: Token generation speed (Tokens/s) and speedup for LLaMA-2 (7B, 13B, 70B) with TGI and SPACE integration on HumanEval-X and MT-Bench datasets under greedy sampling setting.

Method	Batch Size			
	2	4	8	16
AR	22.8	22.1	21.1	19.5
SPACE (k=5)	56.0 (2.46)	49.2 (2.23)	38.4 (1.82)	27.2 (1.39)
SPACE (k=2)	51.8 (2.27)	48.3 (2.19)	41.4 (1.96)	33.9 (1.74)

Table 3: The inference speed in tokens/s per request and speedup for AR and SPACE on MT-Bench dataset. The number in parentheses shows the speedup.

with batches over 8, SPACE with two masks are more efficient than those with five. This is intuitive as a smaller value of  $k$  introduces fewer additional tokens, thereby saving computational resources. More comparisons on AR and SPACE with large batch size can be found in Appendix A.6.

## 5 Conclusion

In this paper, we introduce SPACE, an innovative approach to accelerate inference of LLMs. SPACE is distinguished by 1) its ability to transform an AR LLM into a SAR LLM utilizing SAR-SFT, which is easy to implement as it only requires minor modifications to the dataloader in SFT setup; 2) its unique auto-correct decoding algorithm that enables the same model for both token generation and verification. Experimental results on various LLMs show SPACE can achieve 2.7x-4.0x speedup on HumanEval-X while still preserving model quality.



## 6 Limitations

While SPACE has demonstrated potential in accelerating the inference of LLMs, it also brings about certain limitations that must be acknowledged: First, the primary advantage offered by SPACE is the acceleration of the inference process through the introduction of additional input tokens during decoding, which has the potential to reduce the number of forward passes that LLMs require. However, the presence of these additional tokens inevitably leads to increased computation overhead, notably in terms of FLOPs, when compared to conventional autoregressive decoding. Therefore, it becomes crucial to conduct an exhaustive study on the energy consumption of methods like SPACE, to fully understand and mitigate their ecological impact. The sustainability of deploying such acceleration techniques, considering long-term environmental implications, must factor into the development of responsible AI technologies.

Furthermore, it is important to recognize that the gain in inference speed facilitated by SPACE is variable across different tasks. Our empirical observations suggest that the speedup is inconsistent, and the limited datasets examined in this study could contribute to skewed outcomes. Besides, our evaluations for SPACE were conducted exclusively on English datasets; consequently, the extent to which SPACE can accelerate inference in other languages has not yet been investigated. It is plausible that there are specific datasets where SPACE exhibits a significantly lower degree of acceleration—a scenario not captured within the confines of our experimental array.

Lastly, we leveraged MT-Bench along with a collection of well-established benchmarks, such as MMLU, PIQA, AGIEval, and others, to gauge model performance when trained with SAR-SFT as opposed to traditional SFT methodologies. Despite this extensive set of evaluations, it is critical to emphasize that benchmarking the comprehensive capabilities of LLMs remains a challenge, and the datasets engaged in this research fall short of enabling a definitive judgment. To this end, we advocate for the application of SPACE in diverse downstream tasks by the research community, which will offer a more rounded understanding of its practical utility and limitations.

## References

- Ebtesam Almazrouei, Hamza Alobeidli, Abdulaziz Alshamsi, Alessandro Cappelli, Ruxandra Cojocaru, Merouane Debbah, Etienne Goffinet, Daniel Hestlow, Julien Launay, Quentin Malartic, et al. 2023. Falcon-40b: an open large language model with state-of-the-art performance. *Findings of the Association for Computational Linguistics: ACL*, 2023:10755–10773.
- Jinze Bai, Shuai Bai, Yunfei Chu, Zeyu Cui, Kai Dang, Xiaodong Deng, Yang Fan, Wenbin Ge, Yu Han, Fei Huang, Binyuan Hui, Luo Ji, Mei Li, Junyang Lin, Runji Lin, Dayiheng Liu, Gao Liu, Chengqiang Lu, Keming Lu, Jianxin Ma, Rui Men, Xingzhang Ren, Xuancheng Ren, Chuanqi Tan, Sinan Tan, Jianhong Tu, Peng Wang, Shijie Wang, Wei Wang, Sheng-guang Wu, Benfeng Xu, Jin Xu, An Yang, Hao Yang, Jian Yang, Shusheng Yang, Yang Yao, Bowen Yu, Hongyi Yuan, Zheng Yuan, Jianwei Zhang, Xingxuan Zhang, Yichang Zhang, Zhenru Zhang, Chang Zhou, Jingren Zhou, Xiaohuan Zhou, and Tianhang Zhu. 2023. Qwen technical report. *arXiv preprint arXiv:2309.16609*.
- Luisa Bentivogli, Peter Clark, Ido Dagan, and Danilo Giampiccolo. 2009. The fifth pascal recognizing textual entailment challenge. In *TAC*.
- Yonatan Bisk, Rowan Zellers, Jianfeng Gao, Yejin Choi, et al. 2020. Piqa: Reasoning about physical commonsense in natural language. In *AAAI*, pages 7432–7439.
- Tom Brown, Benjamin Mann, Nick Ryder, Melanie Subbiah, Jared D Kaplan, Prafulla Dhariwal, Arvind Neelakantan, Pranav Shyam, Girish Sastry, Amanda Askell, et al. 2020. Language models are few-shot learners. *Advances in neural information processing systems*, 33:1877–1901.
- Tianle Cai, Yuhong Li, Zhengyang Geng, Hongwu Peng, Jason D. Lee, Deming Chen, and Tri Dao. 2024. Medusa: Simple llm inference acceleration framework with multiple decoding heads. *arXiv preprint arXiv: 2401.10774*.
- Sahil Chaudhary. 2023. Code alpaca: An instruction-following llama model for code generation. <https://github.com/sahil280114/codealpaca>.
- Charlie Chen, Sebastian Borgeaud, Geoffrey Irving, Jean-Baptiste Lespiau, Laurent Sifre, and John Jumper. 2023. Accelerating large language model decoding with speculative sampling. *arXiv preprint arXiv:2302.01318*.
- Christopher Clark, Kenton Lee, Ming-Wei Chang, Tom Kwiatkowski, Michael Collins, and Kristina Toutanova. 2019. Boolq: Exploring the surprising difficulty of natural yes/no questions. In *Proceedings of the 2019 Conference of the North American Chapter of the Association for Computational Linguistics*:

- Human Language Technologies, Volume 1 (Long and Short Papers)*, pages 2924–2936.
- OpenCompass Contributors. 2023. Opencompass: A universal evaluation platform for foundation models. <https://github.com/open-compass/opencompass>.
- Zhengxiao Du, Yujie Qian, Xiao Liu, Ming Ding, Jiezhong Qiu, Zhilin Yang, and Jie Tang. 2022. Glm: General language model pretraining with autoregressive blank infilling. In *Proceedings of the 60th Annual Meeting of the Association for Computational Linguistics (Volume 1: Long Papers)*, pages 320–335.
- Yichao Fu, Peter Bailis, Ion Stoica, and Hao Zhang. 2023. [Breaking the sequential dependency of llm inference using lookahead decoding](#).
- Marjan Ghazvininejad, Omer Levy, Yinhan Liu, and Luke Zettlemoyer. 2019. Mask-predict: Parallel decoding of conditional masked language models. In *Proceedings of the 2019 Conference on Empirical Methods in Natural Language Processing and the 9th International Joint Conference on Natural Language Processing (EMNLP-IJCNLP)*, pages 6112–6121.
- Dan Hendrycks, Collin Burns, Steven Basart, Andy Zou, Mantas Mazeika, Dawn Song, and Jacob Steinhardt. 2020. Measuring massive multitask language understanding. In *International Conference on Learning Representations*.
- hiyouga. 2023. Llama factory. <https://github.com/hiyouga/LLaMA-Factory>.
- HuggingFace. 2023. Large language model text generation inference. <https://github.com/huggingface/text-generation-inference>.
- Joao Gante. 2023. [Assisted generation: a new direction toward low-latency text generation](#).
- Sehoon Kim, Karttikeya Mangalam, Suhong Moon, Jitendra Malik, Michael W Mahoney, Amir Gholami, and Kurt Keutzer. 2023. Speculative decoding with big little decoder. In *Thirty-seventh Conference on Neural Information Processing Systems*.
- Guokun Lai, Qizhe Xie, Hanxiao Liu, Yiming Yang, and Eduard Hovy. 2017. Race: Large-scale reading comprehension dataset from examinations. In *Proceedings of the 2017 Conference on Empirical Methods in Natural Language Processing*, pages 785–794.
- LAION-AI. 2023. Open-assistant. <https://github.com/LAION-AI/Open-Assistant>.
- Ariel N. Lee, Cole J. Hunter, and Nataniel Ruiz. 2023. Platypus: Quick, cheap, and powerful refinement of llms. *arXiv preprint arXiv:2308.07317*.
- Yaniv Leviathan, Matan Kalman, and Yossi Matias. 2023. Fast inference from transformers via speculative decoding. In *International Conference on Machine Learning*, pages 19274–19286. PMLR.
- Feng Lin, Hanling Yi, Hongbin Li, Yifan Yang, Xiaotian Yu, Guangming Lu, and Rong Xiao. 2024. Bit: Bi-directional tuning for lossless acceleration in large language models. *arXiv preprint arXiv:2401.12522*.
- Xiaoxuan Liu, Lanxiang Hu, Peter Bailis, Ion Stoica, Zhijie Deng, Alvin Cheung, and Hao Zhang. 2023. Online speculative decoding. *arXiv preprint arXiv:2310.07177*.
- Xupeng Miao, Gabriele Oliaro, Zhihao Zhang, Xinhao Cheng, Zeyu Wang, Rae Ying Yee Wong, Zhuoming Chen, Daiyaan Arfeen, Reyna Abhyankar, and Zhihao Jia. 2023. Specinfer: Accelerating generative llm serving with speculative inference and token tree verification. *arXiv preprint arXiv:2305.09781*.
- Giovanni Monea, Armand Joulin, and Edouard Grave. 2023. Pass: Parallel speculative sampling. *arXiv preprint arXiv:2311.13581*.
- Shashi Narayan, Shay Cohen, and Maria Lapata. 2018. Don’t give me the details, just the summary! topic-aware convolutional neural networks for extreme summarization. In *2018 Conference on Empirical Methods in Natural Language Processing*, pages 1797–1807. Association for Computational Linguistics.
- Alessandro Palla. 2023. chatbot instruction prompts. [https://huggingface.co/datasets/alespalla/chatbot\\_instruction\\_prompts](https://huggingface.co/datasets/alespalla/chatbot_instruction_prompts).
- Baolin Peng, Chunyuan Li, Pengcheng He, Michel Galley, and Jianfeng Gao. 2023. Instruction tuning with gpt-4. *arXiv preprint arXiv:2304.03277*.
- Pranav Rajpurkar, Robin Jia, and Percy Liang. 2018. Know what you don’t know: Unanswerable questions for squad. In *Proceedings of the 56th Annual Meeting of the Association for Computational Linguistics (Volume 2: Short Papers)*, pages 784–789.
- Jeff Rasley, Samyam Rajbhandari, Olatunji Ruwase, and Yuxiong He. 2020. Deepspeed: System optimizations enable training deep learning models with over 100 billion parameters. In *Proceedings of the 26th ACM SIGKDD International Conference on Knowledge Discovery & Data Mining*, pages 3505–3506.
- Benjamin Frederick Spector and Christopher Ré. 2023. Accelerating llm inference with staged speculative decoding. In *Workshop on Efficient Systems for Foundation Models@ ICML2023*.
- Mitchell Stern, Noam Shazeer, and Jakob Uszkoreit. 2018. Blockwise parallel decoding for deep autoregressive models. *Advances in Neural Information Processing Systems*, 31.

- Ziteng Sun, Ananda Theertha Suresh, Jae Hun Ro, Ahmad Beirami, Himanshu Jain, Felix Yu, Michael Riley, and Sanjiv Kumar. 2023. Spectr: Fast speculative decoding via optimal transport. In *Workshop on Efficient Systems for Foundation Models@ ICML2023*.
- Alon Talmor, Jonathan Herzig, Nicholas Lourie, and Jonathan Berant. 2019. Commonsenseqa: A question answering challenge targeting commonsense knowledge. In *Proceedings of the 2019 Conference of the North American Chapter of the Association for Computational Linguistics: Human Language Technologies, Volume 1 (Long and Short Papers)*, pages 4149–4158.
- Paul Tardy. 2023. Rouge. <https://github.com/pltrdy/rouge>.
- InternLM Team. 2023. Internlm: A multilingual language model with progressively enhanced capabilities. <https://github.com/InternLM/InternLM>.
- Hugo Touvron, Louis Martin, Kevin Stone, Peter Albert, Amjad Almahairi, Yasmine Babaei, Nikolay Bashlykov, Soumya Batra, Prajwal Bhargava, Shruti Bhosale, et al. 2023. Llama 2: Open foundation and fine-tuned chat models. *arXiv preprint arXiv:2307.09288*.
- Chunqi Wang, Ji Zhang, and Haiqing Chen. 2018. Semi-autoregressive neural machine translation. In *Proceedings of the 2018 Conference on Empirical Methods in Natural Language Processing*, pages 479–488.
- Thomas Wolf, Lysandre Debut, Victor Sanh, Julien Chaumond, Clement Delangue, Anthony Moi, Pierric Cistac, Tim Rault, Rémi Louf, Morgan Funtowicz, Joe Davison, Sam Shleifer, Patrick von Platen, Clara Ma, Yacine Jernite, Julien Plu, Canwen Xu, Teven Le Scao, Sylvain Gugger, Mariama Drame, Quentin Lhoest, and Alexander M. Rush. 2020. **Transformers: State-of-the-art natural language processing**. In *Proceedings of the 2020 Conference on Empirical Methods in Natural Language Processing: System Demonstrations*, pages 38–45, Online. Association for Computational Linguistics.
- Heming Xia, Tao Ge, Furu Wei, and Zhifang Sui. 2022. Lossless speedup of autoregressive translation with generalized aggressive decoding. *arXiv preprint arXiv:2203.16487*.
- Yisheng Xiao, Lijun Wu, Junliang Guo, Juntao Li, Min Zhang, Tao Qin, and Tie-yan Liu. 2023. A survey on non-autoregressive generation for neural machine translation and beyond. *IEEE Transactions on Pattern Analysis and Machine Intelligence*.
- Rowan Zellers, Ari Holtzman, Yonatan Bisk, Ali Farhadi, and Yejin Choi. 2019. Hellaswag: Can a machine really finish your sentence? In *Proceedings of the 57th Annual Meeting of the Association for Computational Linguistics*.
- Jun Zhang, Jue Wang, Huan Li, Lidan Shou, Ke Chen, Gang Chen, and Sharad Mehrotra. 2023. Draft & verify: Lossless large language model acceleration via self-speculative decoding. *arXiv preprint arXiv:2309.08168*.
- Lianmin Zheng, Wei-Lin Chiang, Ying Sheng, Siyuan Zhuang, Zhanghao Wu, Yonghao Zhuang, Zi Lin, Zhuohan Li, Dacheng Li, Eric Xing, et al. 2023a. Judging llm-as-a-judge with mt-bench and chatbot arena. *arXiv preprint arXiv:2306.05685*.
- Qinkai Zheng, Xiao Xia, Xu Zou, Yuxiao Dong, Shan Wang, Yufei Xue, Zihan Wang, Lei Shen, Andi Wang, Yang Li, Teng Su, Zhilin Yang, and Jie Tang. 2023b. Codegex: A pre-trained model for code generation with multilingual evaluations on humaneval-x.
- Wanjun Zhong, Ruixiang Cui, Yiduo Guo, Yaobo Liang, Shuai Lu, Yanlin Wang, Amin Saied, Weizhu Chen, and Nan Duan. 2023. Agieval: A human-centric benchmark for evaluating foundation models.
- Chunting Zhou, Pengfei Liu, Puxin Xu, Srinu Iyer, Jiao Sun, Yuning Mao, Xuezhe Ma, Avia Efrat, Ping Yu, Lili Yu, et al. 2023. Lima: Less is more for alignment. *arXiv preprint arXiv:2305.11206*.

## A Appendix

### A.1 Training Details

We conduct all our experiments on a cluster of 4 servers, where each server is equipped with eight A800 (80G) GPUs. We adopt distinct training strategies based on the size of the models being trained. For models with fewer than 14 billion parameters, we allocate our experiments to a single server and employ the ZeRO-2 (Rasley et al., 2020) optimization for distributed training. Conversely, for models that exceed the 14 billion parameter mark, we expand our setup to utilize all four servers and implement the ZeRO-3 optimization to effectively handle the increased computational demands. We adopt LLaMA Factory (hiyouga, 2023) to fine-tune the LLMs. The specific hyper-parameters utilized for the SAR-SFT are documented and can be referenced in Table 4.

Table 5 shows the statistics of SFT datasets used to finetune the models. Note that all the dataset are publicly available. The fine-tuning duration for LLMs can vary significantly based on the size of the model and the computational resources available. For the LLaMA-2-7B model, the fine-tuning process typically takes about 6 hours on a server equipped with eight A800 (80GB) GPUs. For the largest variant, the LLaMA-2-70B, the SAR-SFT requires roughly 18 hours to complete using 4

Hyper-parameters	Value
max source tokens	2048
max target tokens	2048
learning rate	5e-5
scheduler	cosine
Adam $\beta_1$	0.9
Adam $\beta_2$	0.999
epoch	2
per device batch size	4
gradient clip	1.0

Table 4: Hyper-parameters and training configurations of SAR-SFT.

servers, each equipped with 8 A800 (80GB) GPUs (totalling 32 GPUs).

We observe that the introduction of SAR-SFT imposes negligible additional training costs when compared to conventional SFT. This is largely due to the minimal intervention in the training process: we only inject  $k = 5$  additional mask tokens during SAR-SFT training. Specifically, the adaptation concerns solely the dataloader—other components are kept consistent with the standard SFT approach. In this modified dataloader, each data sample remains unchanged with a probability  $p_{ar}$ . Conversely, with a probability of  $1 - p_{ar}$ , we randomly select a position  $m$  in the input sequence to replace  $k$  consecutive tokens with mask tokens, while the label sequence is left intact. We then truncate the input and label token sequences to keep the first  $m + k$  tokens. Compared to the standard SFT, which does not employ truncation on the training sample, the training cost of SAR-SFT is marginally reduced, as tokens beyond the positions  $m + k$  are discarded during the training process in SAR-SFT. Namely, SAR-SFT actually sees less tokens during training than SFT. Empirical evidence from our experiments supports this assertion, as we recorded similar training durations for both SAR-SFT and SFT under identical training configurations.

## A.2 Evaluation Details

We performed our inference experiments on a server equipped with eight A800 (80GB) GPUs. For models with fewer than 14 billion parameters, inference is conducted using a single GPU. For larger models, those with parameters exceeding 14B, we employ multiple GPUs and leverage tensor parallelism to manage the increased computational load effectively. During the inference process, we

configure our setup with a batch size of one to ensure precise measurement of inference latency on a per-instance basis.

In our experiment, we employ four distinct datasets: Chatbot Instruction Prompt (CIP) (Palla, 2023), MT-Bench (Zheng et al., 2023a), HumanEval-X (Zheng et al., 2023b) and XSum (Narayan et al., 2018). CIP is a conversational dataset from which we utilize prompts to simulate realistic conversations. MT-Bench is a dataset comprised of multi-turn questions, encompassing a wide range of topics. HumanEval-X is a standard benchmark for Python code generation and Pass@10 is used as the metric. Lastly, the XSum dataset, which tasks models with summary generation, is evaluated using ROUGE-L.

For generation tasks, we tailored specific prompt templates to guide the model’s output. When working with the XSum dataset, we used the following prompt template: “Document: {TEXT}\n Based on the previous text, provide a brief single summary”. Similarly, for the HumanEval-X dataset, which is designed for code generation, we employed the prompt template as follows: “Complete the following python code. Do not give any explanation or testing examples, just complete the code.\n {TEXT}”. For CIP and MT-Bench, we do not use any prompt template.

To measure the performance of LLMs on XSum and HumanEval-X, we compute the ROUGE-L and Pass@10, respectively. The ROUGE-L is calculated using python package rouge (Tardy, 2023) and the pass@10 is computed using official evaluation script (Zheng et al., 2023b).

The inference speedup for each task within the MT-Bench benchmark under greedy sampling setting across various models are shown in Table 6.

## A.3 Attention Mask in SPACE

An illustrative example of the attention mask is shown in Figure 7. The attention mask used in SPACE is tailored such that masked tokens can causally attend only to other mask tokens within the same group and to preceding non-masked tokens. Furthermore, all non-masked tokens are restricted to causally attend to prior non-masked tokens, and are unable to attend to any preceding masked tokens.

## A.4 Random Sampling

To rigorously evaluate model performance on the XSum and HumanEval-X datasets with random



Dataset	Language	Sample Numbers	Average Input Tokens	Average Output Tokens
Alpaca-GPT4-zh (Peng et al., 2023)	zh	48,818	30.9	292.5
Alpaca-GPT4-en (Peng et al., 2023)	en	52,002	21.6	162.6
LIMA (Zhou et al., 2023)	en	1,029	74.2	639.1
Oaast-SFT (LAION-AI, 2023)	multi	20,202	198.8	234.8
CodeAlpaca (Chaudhary, 2023)	en	20,022	28.8	68.6
OpenPlatypus (Lee et al., 2023)	en	24,926	159.6	225.3

Table 5: Statistics of SFT datasets used to finetuned the models. The average input tokens and output tokens are calculated using LLaMA-2-7B tokenizer.

Model	Code	Extraction	Humanities	Math	Reasoning	Role-play	Stem	Writing	Overall
ChatGLM-3-6B	2.83	3.35	1.91	2.54	1.87	1.98	2.03	2.43	2.32
LLaMA-2-7B	2.14	3.12	1.96	2.61	1.83	1.89	1.65	2.25	2.19
LLaMA-2-13B	2.89	3.66	2.20	2.99	2.29	2.03	2.27	2.68	2.53
Qwen-14B	2.88	3.76	2.18	2.85	2.04	1.86	2.05	2.55	2.43
InternLM-20B	2.50	3.28	2.05	3.55	1.89	2.00	2.02	2.05	2.36
Falcon-40B	2.02	2.90	1.72	2.22	1.69	1.53	1.69	1.76	2.17
LLaMA-2-70B	2.61	3.70	1.97	3.03	2.50	1.73	1.84	2.09	2.26

Table 6: The experimental results on MT-Bench under greedy sampling setting. We show the inference speedup for each task in MT-Bench.

	LLMs	are	[M]	[M]	auto	[M]	[M]	model	[M]	[M]
LLMs	1									
are	1	1								
[M]	1	1	1							
[M]	1	1	1	1						
auto	1	1			1					
[M]	1	1			1	1				
[M]	1	1			1	1	1			
model	1	1			1			1		
[M]	1	1			1			1	1	
[M]	1	1			1			1	1	1

Figure 7: An illustrative example of the attention mask used in SPACE. In this example,  $k = 2$  and the input is extended with 8 tokens. “LLMs are” are the input query, “auto” and “model” are two candidate tokens that need to be verified.

sampling enabled <sup>2</sup>, we conducted ten runs of the evaluation process to counteract the influence

<sup>2</sup>When using random sampling, we set top-p=0.95 and top-k=10

of randomness. The mean and variance of these runs are reported in Table 7. Under random sampling setting, the performance metrics for SPACE and the baseline are similar on both XSum and HumanEval-X, as presented in Table 7. This consistency across multiple evaluations confirms the distributional alignment between SPACE and the baseline model under the random sampling setting.

### A.5 SAR-SFT versus SFT

To further demonstrate that SAR-SFT does not impede the model’s performance, we compared the performance of LLaMA-2 (with model sizes of 7B, 13B, and 70B parameters) trained with both SAR-SFT and traditional SFT. The comparison spanned a suite of widely used benchmarks, which we have categorized into the following four groups:

- **Academic.** We report the average accuracy of the model on the MMLU (Hendrycks et al., 2020) and AGIEval (Zhong et al., 2023) benchmarks.
- **Knowledge.** We evaluate the model on CommonSenseQA (Talmor et al., 2019) and BoolQ (Clark et al., 2019), reporting their average results.

Model	XSum			HumanEval-X		
	ROUGE-L	Avg. Tokens	Speedup	Pass@10	Avg. Tokens	Speedup
ChatGLM-3-6B	14.8 ± 0.2 (14.0 ± 0.4)	1.95 ± 0.01	1.47 ± 0.01	23.2 (22.8)	3.16 ± 0.04	2.09 ± 0.08
LLaMA-2-7B	15.1 ± 0.2 (15.3 ± 0.1)	2.14 ± 0.02	1.79 ± 0.04	18.9 (18.3)	3.56 ± 0.05	2.86 ± 0.04
LLaMA-2-13B	15.2 ± 0.2 (15.6 ± 0.2)	2.24 ± 0.01	1.86 ± 0.02	31.7 (32.3)	4.15 ± 0.02	3.81 ± 0.05
Qwen-14B	16.1 ± 0.3 (16.3 ± 0.3)	2.05 ± 0.01	1.91 ± 0.04	32.3 (31.7)	3.09 ± 0.04	2.86 ± 0.04
InternLM-20B	16.3 ± 0.2 (17.0 ± 0.2)	1.99 ± 0.01	1.73 ± 0.01	25.0 (23.7)	3.13 ± 0.03	2.67 ± 0.08
Falcon-40B	16.6 ± 0.2 (15.4 ± 0.3)	2.09 ± 0.04	2.08 ± 0.03	27.4 (28.0)	3.42 ± 0.03	2.88 ± 0.06
LLaMA-2-70B	16.1 ± 0.2 (16.2 ± 0.3)	2.40 ± 0.02	2.25 ± 0.02	36.6 (38.2)	4.15 ± 0.02	3.81 ± 0.05

Table 7: The experimental results on XSum and HumanEval-X using random sampling. We show the mean and variance (over 10 runs) of the average accepted tokens (Avg. Tokens) and inference speedup (Speedup) for each datasets. The number in parentheses shows the corresponding results of the baseline method.

- **Reasoning.** We assess the 5-shot performance on PIQA (Bisk et al., 2020), RTE (Bentivogli et al., 2009) and HellaSwag (Zellers et al., 2019), reporting their mean performance.
- **Understanding.** We report the average result on RACE (Lai et al., 2017) and SQuAD2.0 (Rajpurkar et al., 2018).

The evaluations were conducted using OpenCompass (Contributors, 2023), an opensource platform designed for large language model evaluation. Comparative performance results are detailed in Table 8. Upon examination of the results, we note small discrepancies between the models fine-tuned with the two distinct training schemes across different tasks.

### A.6 Discussion on Large Batch Size

When operating at the same batch sizes, SPACE consumes more GPU computational resources to speed up inference in comparison to AR. Nevertheless, with an increase in batch size, the GPU becomes compute-bound, effectively neutralizing SPACE’s performance advantage. To provide a fair assessment of SPACE and AR, we perform experiments on the XSum dataset for both methods. Our focus is on evaluating their throughput, defined as the number of output tokens per second that an inference server can produce across all

requests, while experimenting with various batch sizes. The findings, illustrated in Figure 8, reveal that SPACE’s throughput significantly diminishes when compared to AR at larger batch sizes. Specifically, the throughput for SPACE plateaus when the batch size reaches approximately 64, whereas AR’s throughput does not saturate until around a batch size of 128. However, SPACE remains competitive at lower batch sizes. Notably, with batch sizes smaller than 16, SPACE’s throughput exceeds that of AR.

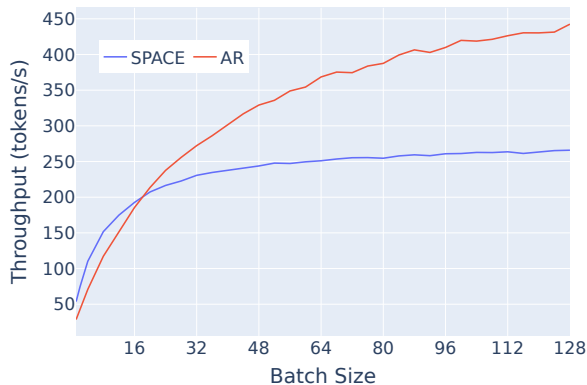


Figure 8: Throughput of SPACE and AR under various batch sizes on XSum dataset.

Furthermore, it is worth noting that many practical applications, especially those on edge devices, often operate with a small batch size. In such cases, the inference process remains memory-

<b>Model</b>	<b>Scheme</b>	<b>Academic</b>	<b>Knowledge</b>	<b>Reasoning</b>	<b>Understanding</b>
LLaMA-2-7B	SAR-SFT	35.4	66.1	62.3	37.2
	SFT	36.0	65.9	64.1	38.6
LLaMA-2-13B	SAR-SFT	40.9	69.4	66.7	55.2
	SFT	40.5	71.4	65.2	57.4
LLaMA-2-70B	SAR-SFT	50.6	76.7	68.4	64.7
	SFT	51.7	77.2	68.0	66.7

Table 8: Performance comparison of LLaMA-2 (7B, 13B, 70B) with different training schemes.

bound rather than compute-bound. SPACE can effectively utilize the available computing resources to enhance the inference speed in low batch size scenarios, making it an attractive and valuable solution for such use cases.